LRRK2 and its substrate Rab GTPases are sequentially targeted onto stressed lysosomes and maintain their homeostasis

Tomoya Eguchi[a,1], Tomoki Kuwahara[a,1], Maria Sakurai[a,1], Tadayuki Komori[a], Tetta Fujimoto[a], Genta Ito[b], Shin-ichiro Yoshimura[c], Akihiro Harada[c], Mitsunori Fukuda[d], Masato Koike[e], and Takeshi Iwatsubo[a,2]

[a]Department of Neuropathology, Graduate School of Medicine, The University of Tokyo, 113-0033 Tokyo, Japan; [b]Laboratory of Brain and Neurological Disorders, Graduate School of Pharmaceutical Sciences, The University of Tokyo, 113-0033 Tokyo, Japan; [c]Department of Cell Biology, Graduate School of Medicine, Osaka University, 565-0871 Osaka, Japan; [d]Laboratory of Membrane Trafficking Mechanisms, Department of Integrative Life Sciences, Graduate School of Life Sciences, Tohoku University, 980-8578 Sendai, Japan; and [e]Department of Cell Biology and Neuroscience, Juntendo University Graduate School of Medicine, 113-8421 Tokyo, Japan

Edited by Peter J. Novick, University of California, San Diego, La Jolla, CA, and approved August 15, 2018 (received for review July 25, 2018)

Leucine-rich repeat kinase 2 (*LRRK2*) has been associated with a variety of human diseases, including Parkinson's disease and Crohn's disease, whereas *LRRK2* deficiency leads to accumulation of abnormal lysosomes in aged animals. However, the cellular roles and mechanisms of LRRK2-mediated lysosomal regulation have remained elusive. Here, we reveal a mechanism of stress-induced lysosomal response by LRRK2 and its target Rab GTPases. Lysosomal overload stress induced the recruitment of endogenous LRRK2 onto lysosomal membranes and activated LRRK2. An upstream adaptor Rab7L1 (Rab29) promoted the lysosomal recruitment of LRRK2. Subsequent family-wide screening of Rab GTPases that may act downstream of LRRK2 translocation revealed that Rab8a and Rab10 were specifically accumulated on overloaded lysosomes dependent on their phosphorylation by LRRK2. Rab7L1-mediated lysosomal targeting of LRRK2 attenuated the stress-induced lysosomal enlargement and promoted lysosomal secretion, whereas Rab8 stabilized by LRRK2 on stressed lysosomes suppressed lysosomal enlargement and Rab10 promoted lysosomal secretion, respectively. These effects were mediated by the recruitment of Rab8/10 effectors EHBP1 and EHBP1L1. LRRK2 deficiency augmented the chloroquine-induced lysosomal vacuolation of renal tubules in vivo. These results implicate the stress-responsive machinery composed of Rab7L1, LRRK2, phosphorylated Rab8/10, and their downstream effectors in the maintenance of lysosomal homeostasis.

LRRK2 | lysosome | Rab GTPase | phosphorylation

The leucine-rich repeat kinase 2 (*LRRK2*) gene encodes a large protein kinase harboring multiple functional domains, including GTP-binding and kinase domains. Missense mutations in *LRRK2* cause the autosomal-dominantly inherited form of Parkinson's disease (PD), a common neurodegenerative disorder of the central nervous system (1, 2). Furthermore, genome-wide association studies have linked common genetic variants at the *LRRK2* locus to sporadic PD (3), as well as inflammatory bowel disease (4) and leprosy (5). LRRK2 is expressed in various organs, including brain, kidney, lung, and immune tissues (6, 7), and the expression is potently induced by IFN-γ treatment (8). LRRK2 may thus serve functions in a broad range of tissues and cell types, including neurons and immune cells.

Previous studies have implicated the role of LRRK2 in a wide variety of cellular events, including vesicular trafficking, cytoskeletal function, autophagy, and the regulation of the endolysosomal system (9, 10). Among these, the role of LRRK2 in the lysosomal system is highlighted because aged *Lrrk2* knockout (KO) mice exhibited an accumulation of enlarged secondary lysosomes containing autofluorescent lipofuscin in renal proximal tubules and lamellar bodies in lung type II cells (11–13). A similar lung phenotype was observed in nonhuman primates treated with LRRK2 kinase inhibitors (14). However, the roles of LRRK2 in the lysosomal system, especially those related to its kinase activity, are yet to be elucidated.

Cell-based studies have implicated LRRK2 in the endolysosomal vesicular trafficking that involves the Rab family of small GTPases (15, 16). One of these Rab GTPases, Rab7L1 (also known as Rab29), has been shown to function in vivo in the maintenance of lysosomes in renal proximal tubule cells (17). *Rab7L1* is also a candidate PD risk gene located within the *PARK16* locus (18–20), and the variants in *LRRK2* and *PARK16* impact PD risk in a nonadditive manner (15, 21). Recent studies have suggested that Rab7L1 recruits LRRK2 to the *trans*-Golgi network and up-regulates its kinase activity (22, 23).

Notably, recent studies have identified a subset of Rab GTPases, including Rab3, Rab8, Rab10, Rab35, and Rab7L1, as bona fide substrates of LRRK2 in cells (22, 24–26). LRRK2 phosphorylates the Thr72 residue in Rab8 and the structurally equivalent residues in other substrate Rab GTPases, and, importantly, the LRRK2-mediated phosphorylation is significantly enhanced

Significance

LRRK2, a protein kinase related to Parkinson's disease, is implicated in the maintenance of lysosomes, and a subset of Rab GTPases has been identified as bona fide substrates of LRRK2. Here, we reveal a key stress-responsive pathway composed of Rab7L1, LRRK2, and phosphorylated Rab8/10 involved in lysosomal homeostasis. Lysosomal overload stress induces translocation of Rab7L1 and LRRK2 to lysosomes, where LRRK2 is activated, and stabilizes Rab8 and Rab10 through phosphorylation. The activation of this machinery protects against lysosomal enlargement and upregulates lysosomal secretion through Rab effectors, EHBP1 and EHBP1L1. These findings elucidate a novel regulatory mechanism of Rab GTPases by phosphorylation by LRRK2 in stressed lysosomes, which may also be involved in the pathomechanism of LRRK2-related disorders.

Author contributions: T.E., T. Kuwahara, and T.I. designed research; T.E., T. Kuwahara, M.S., T. Komori, T.F., G.I., and M.K. performed research; G.I., S.-i.Y., A.H., and M.F. contributed new reagents/analytic tools; T.E., T. Kuwahara, M.S., M.K., and T.I. analyzed data; and T.E., T. Kuwahara, and T.I. wrote the paper.

The authors declare no conflict of interest.

This article is a PNAS Direct Submission.

[1]T.E., T. Kuwahara, and M.S. contributed equally to this work.

[2]To whom correspondence should be addressed. Email: iwatsubo@m.u-tokyo.ac.jp.

This article contains supporting information online at www.pnas.org/lookup/suppl/doi:10.1073/pnas.1812196115/-/DCSupplemental.

Published online September 12, 2018.

by the PD-associated LRRK2 mutations (22, 24–26). The LRRK2-mediated phosphorylation of Rab GTPases may negatively regulate their functions in certain cellular contexts: Phosphorylation of Rab8a suppressed ciliogenesis (25) or centrosomal cohesion (27), and that of Rab7L1 affected the *trans*-Golgi morphology (26). Rab GTPases cycle between inactive GDP-bound and active GTP-bound states, which is regulated by their interactors, guanine nucleotide exchange factors (GEFs) and GTPase-activating proteins (GAPs). Prior studies have suggested that Rab phosphorylation abolished their interaction with GDP dissociation inhibitors (GDI1/2) (24, 27). Thus, a precise understanding of the cellular roles of Rab phosphorylation in the physiological and disease-related contexts is imperative.

In this study, we reveal a stress-responsive behavior of LRRK2 and its target Rab GTPases. Upon lysosomal overload stress, LRRK2 was activated and readily recruited onto lysosomes. Rab7L1 acted as an upstream adaptor to facilitate LRRK2 translocation. LRRK2 then stabilized Rab8 and Rab10 on lysosomes depending on their phosphorylation, and Rab7L1, LRRK2, Rab8/10, and their effectors, EH domain-binding protein 1 (EHBP1) and EHBP1-like 1 (EHBP1L1), were altogether involved in the regulation of stress-induced lysosomal enlargement and secretion. Our present results underscore the roles of LRRK2 and related Rab GTPases in the maintenance of lysosomal homeostasis.

Results

LRRK2 Is Recruited onto the Enlarged Lysosomes upon Treatment with Chloroquine. We first investigated the detailed subcellular localization of endogenous LRRK2 in various cell types that express a high level of LRRK2, including 3T3-Swiss albino fibroblasts, mouse macrophage RAW264.7 cells, and mouse microglia MG6 cells, in addition to HEK293 cells overexpressing 3× FLAG-tagged LRRK2. LRRK2 was predominantly distributed throughout the cytoplasm (Fig. 1 *A* and *C*), consistent with previous findings (28–31), whereas a small proportion of cells (~0.1–1% of total) exhibited an accumulation of LRRK2 on enlarged lysosomes that were positive for a lysosomal marker, LAMP1 (*SI Appendix*, Fig. S1*A*).

To examine whether LRRK2 is recruited onto enlarged lysosomes, we treated cells with chloroquine (CQ), a lysosomotropic agent that causes the enlargement of lysosomes by accumulating within lysosomal lumens. We found that CQ treatment readily induced the relocalization of LRRK2 onto enlarged lysosomes (Fig. 1 *B* and *D* and *SI Appendix*, Fig. S1 *B–D*). The recruitment of LRRK2 was observed in all types of cells examined, but the efficiency and the speed were different: ~50% of RAW264.7 cells exhibited LRRK2 recruitment after 1–3 h of CQ treatment, whereas the efficiency was much lower (~15%) in 3T3 and MG6 cells, and a 24-h CQ treatment recruited LRRK2 to lysosomes in transfected HEK293 cells (*SI Appendix*, Fig. S1*D*). The specificity of the LRRK2 immunoreactivities was confirmed using three well-characterized antibodies (*SI Appendix*, Fig. S2 *A–C*). The lysosomal enlargement was induced after 30 min of CQ treatment, whereas LRRK2 translocation to lysosomes was observed at 60 min, suggesting that translocation of LRRK2 occurs after lysosomes become enlarged (Fig. 1 *E* and *F*). The protein expression levels of LRRK2 and LAMP1 were not altered by CQ treatment (*SI Appendix*, Fig. S2 *D–F*).

We then examined the lysosomal localization of LRRK2 at an ultrastructural level by immunoelectron microscopy (IEM). We

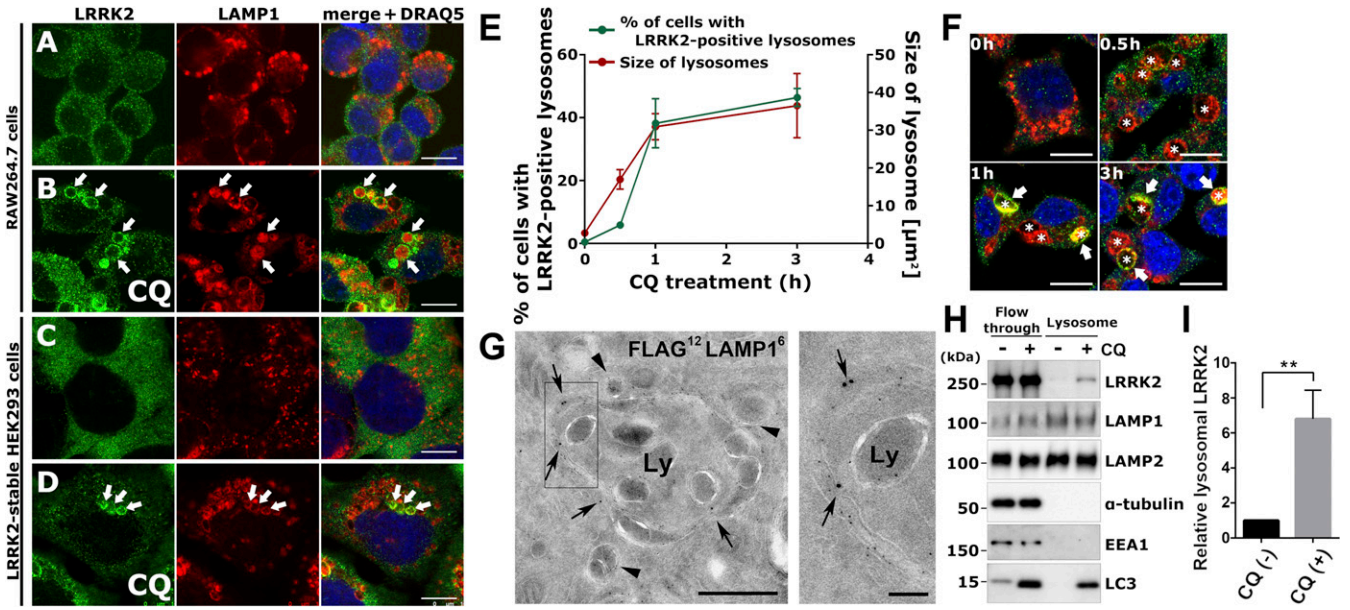

Fig. 1. LRRK2 is recruited onto the enlarged lysosomes. Immunocytochemical analysis of subcellular localization of LRRK2 using an anti-LRRK2 antibody MJFF2 (*A* and *B*, green) or an anti-FLAG antibody (*C* and *D*, green) is shown. Lysosomes were stained with an anti-LAMP1 antibody (red), and nuclei were stained with DRAQ5 (blue). RAW264.7 cells without (*A*) or with (*B*) CQ treatment (50 μM, 3 h) are shown. The 3× FLAG-LRRK2-stable HEK293 cells without (*C*) or with (*D*) CQ treatment (50 μM, 24 h) are shown. Arrows represent LRRK2-positive enlarged lysosomes. (Scale bars: *A–D*, 10 μm.) (*E*) Percentages of RAW264.7 cells harboring LRRK2-positive lysosomes and the size of lysosomes were analyzed. Data represent mean ± SEM [$n = 3$, 91–148 cells were analyzed in each experiment (percentage of cells with LRRK2-positive lysosomes)]; mean ± SD [$n = 20$ cells (size of lysosomes)]. (*F*) Representative photographs at each time point analyzed in *E*. Green, LRRK2; red, LAMP1; blue, DRAQ5; asterisks, the enlarged lysosomes; arrows, LRRK2-positive lysosomes. (Scale bars: 10 μm.) (*G*) IEM analysis of the enlarged lysosomes using ultrathin cryosections of the CQ-treated bone marrow-derived macrophages isolated from FLAG-LRRK2 BAC transgenic mice. The 12-nm gold particles indicate FLAG-LRRK2 (arrows) and the 6-nm gold particles indicate LAMP1. Ly, enlarged lysosome. Arrowheads indicate normal lysosomes. A higher magnification (*Right*) of the boxed area (*Left*) is shown. (Scale bars: *Right*, 100 nm; *Left*, 500 nm). (*H*) The levels of LRRK2 and control proteins in the lysosomal fraction analyzed by immunoblotting. Lysosomes were magnetically isolated from HEK293 cells expressing 3× FLAG-LRRK2 with or without CQ treatment. LC3-II induction was examined to validate the effectiveness of CQ. (*I*) Levels of LRRK2 in the lysosomal fraction analyzed in *H*. The LRRK2 levels were normalized by the levels of LAMP2. Data represent mean ± SD ($n = 3$). $^{**}P < 0.01$, *t* test.

analyzed CQ-treated primary macrophages from FLAG-LRRK2 (G2019S) BAC transgenic mice, in which LRRK2 translocation to lysosomes could easily be assessed (*SI Appendix*, Fig. S2*G*). IEM analysis revealed that FLAG-LRRK2 was detected selectively on the outer surface of membranes of enlarged lysosomes, whereas LAMP1 was massively immunolabeled on membranes of enlarged lysosomes as well as on those of vacuolar structures accumulating within lysosomes (Fig. 1*G*).

To biochemically verify the LRRK2 translocation to lysosomes, we purified the lysosomes by the superparamagnetic chromatography isolation method (32, 33). HEK293 cells expressing LRRK2 were cultured in media containing iron-dextran, which were internalized and accumulated within lysosomes, and the lysosomes were then magnetically isolated. Immunoblot analysis revealed that CQ treatment significantly increased the levels of LRRK2 in the lysosomal fraction (Fig. 1 *H* and *I*). These results indicated that LRRK2 is recruited onto the enlarged lysosomes.

Lysosomal Overload Induces Translocation and Activation of LRRK2. CQ-induced lysosomal stresses include lysosomal overload, neutralization of luminal pH, and enlargement of lysosomes. To determine which specific stress induces LRRK2 translocation onto lysosomes, we treated RAW264.7 cells with a set of different lysosomal stressors other than CQ (Fig. 2 *A* and *B*). We first treated cells with bafilomycin A1 (BafA1), an inhibitor of lysosomal V-ATPase; acute treatment with BafA1 (<3 h) neutralizes lysosomal pH without inducing lysosomal overload or enlargement. Treatment with BafA1 for 1–3 h completely abolished the lysosomal acidity (*SI Appendix*, Fig. S3*A*), whereas the translocation of LRRK2 was not observed (Fig. 2 *C* and *F*). We also exposed cells to vacuolin-1, a compound that causes lysosomal enlargement without inducing lysosomal overload (34). Lysosomes were enlarged in vacuolin-1–treated cells, whereas LRRK2 was not recruited (Fig. 2 *D* and *F*). Treatment with hydrogen peroxide, which causes oxidative stress and resultant lysosomal deterioration or rupture (35), did not induce LRRK2 recruitment either (*SI Appendix*, Fig. S3*B*). These results suggested that an increase in luminal pH, lysosomal enlargement, and oxidative stress are not triggers for the LRRK2 translocation.

To examine whether CQ-induced translocation of LRRK2 is a result of CQ accumulation in lysosomes, we treated cells with CQ in the presence of BafA1, which prevents CQ accumulation by neutralizing lysosomal pH. Treatment of cells with both reagents prevented LRRK2 translocation (Fig. 2 *E* and *F*). Similar to the CQ treatment, prolonged exposure to BafA1 is expected to induce lysosomal overload through accumulation of endogenous substrates. Treatment of cells with BafA1 for 6–12 h caused a time-dependent induction of the endogenous LRRK2 translocation to

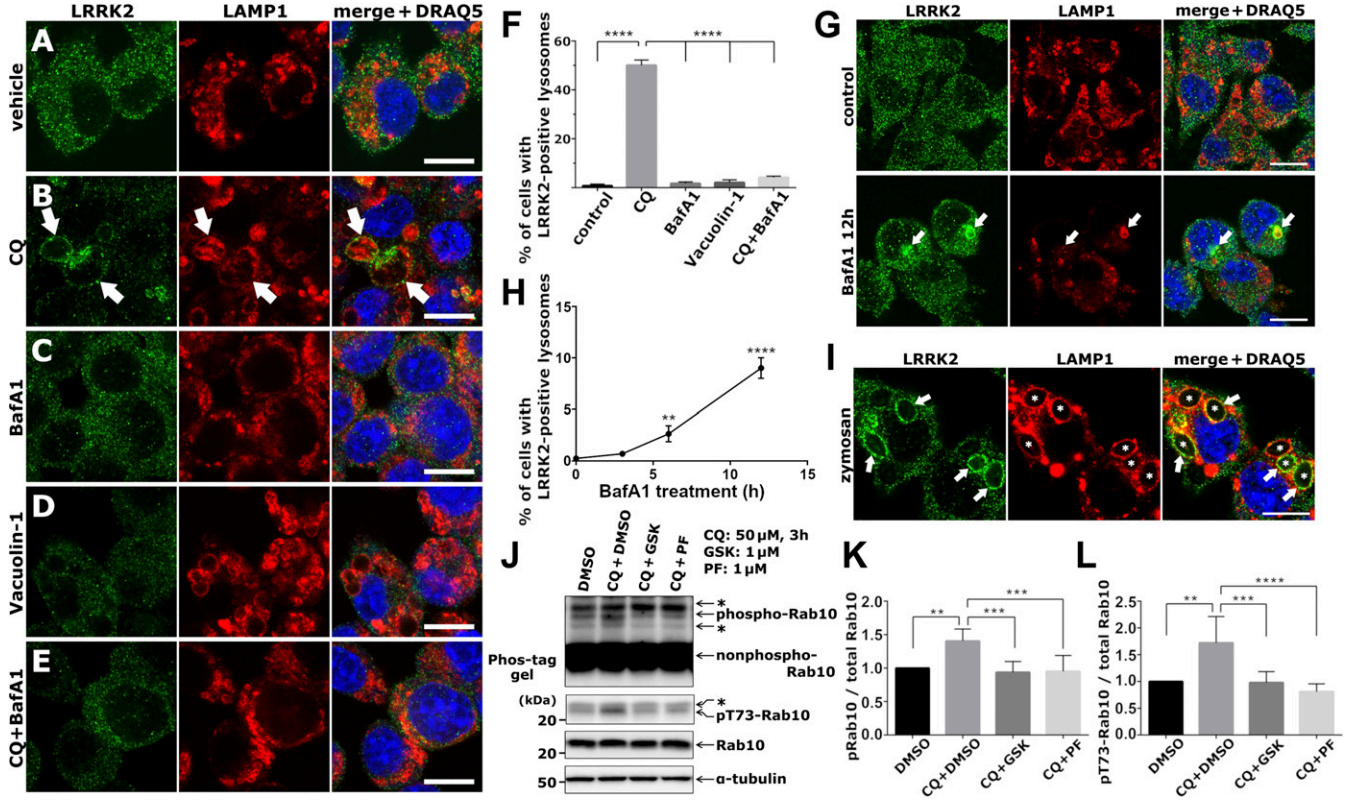

Fig. 2. Lysosomal overload induces translocation and activation of LRRK2. (*A*–*E*) Lysosomal localization of LRRK2 was analyzed in RAW264.7 cells treated with the indicated reagents for 3 h. Vehicle (*A*), CQ (*B*, 50 μM), BafA1 (*C*, 100 nM), vacuolin-1 (*D*, 500 nM), and CQ plus BafA1 (*E*, 50 μM and 100 nM, respectively) are shown. (Scale bars: *A*–*E*, 10 μm.) (*F*) Percentages of cells harboring LRRK2-positive lysosomes exposed to each indicated reagent as shown in *A*–*E*. Data represent mean ± SEM (n = 3, 171–390 cells were analyzed in each experiment). ****$P < 0.0001$, one-way ANOVA with Tukey's test. (*G*) Lysosomal localization of LRRK2 in RAW264.7 cells treated with BafA1 (100 nM) for 12 h. Arrows indicate LRRK2-positive lysosomes. (Scale bars: 10 μm.) (*H*) Percentages of cells harboring LRRK2-positive lysosomes analyzed at 0, 3, 6, or 12 h of BafA1 exposure. Mean ± SEM (n = 4, 112–454 cells were analyzed at each time point). **$P < 0.01$, ****$P < 0.0001$; t test compared with $t = 0$ h. (*I*) Localization of endogenous LRRK2 on phagolysosomes in RAW264.7 cells fed with zymosan for 1 h. Arrows represent LRRK2-positive phagolysosomes, and asterisks represent phagolysosomes containing zymosan. (Scale bar: 10 μm.) (*J*) Levels of phosphorylated Rab10 in RAW264.7 cells analyzed by Phos-tag SDS/PAGE using an anti-Rab10 antibody or by standard SDS/PAGE using an anti–phospho-Rab10 (pThr73) antibody. Asterisks represent nonspecific bands. Densitometric analysis of the levels of phosphorylated Rab10, as shown in *J*, analyzed by Phos-tag SDS/PAGE using anti-Rab10 antibody (*K*) or by standard SDS/PAGE using anti–phospho-Rab10 (pThr73) antibody (*L*) are shown. **$P < 0.01$, ***$P < 0.001$, ****$P < 0.0001$, one-way ANOVA with Tukey's test.

the enlarged lysosomes (Fig. 2 *G* and *H*). We further tested the LRRK2 translocation upon treatment with zymosan, a yeast cell-wall preparation that is readily internalized into phagolysosomes, loading osmotic stress in phagocytic cells (36, 37). Treatment of RAW264.7 cells with zymosan induced the translocation of LRRK2 on newly formed phagolysosomes [~10–20% of phagolysosomes were positive for LAMP1 (Fig. 2*I*)]. LRRK2 on lysosomes/phagolysosomes was colocalized with LC3, a marker of stressed lysosomes (37), as well as autophagosomal double-membrane structures (*SI Appendix*, Fig. S3*C*). These results collectively suggest that the lysosomal overload stress induces LRRK2 translocation.

We further examined whether lysosomal overload stress alters the kinase activity of endogenous LRRK2 to phosphorylate Rab10, a well-validated substrate of LRRK2 (24, 38). We performed Phos-tag SDS/PAGE analysis, which enables separation of phosphorylated proteins in Phos-tag–containing gels (39). Phosphorylation of endogenous Rab10 was significantly increased by CQ treatment (Fig. 2 *J* and *K*). The increase in Rab10 phosphorylation occurred at the Thr73 residue, a target site of LRRK2 (Fig. 2 *J* and *L*). Treatment with either of the LRRK2-specific kinase inhibitors, GSK2578215A (GSK) (40) or PF-06447475 (PF) (41), suppressed the CQ-induced phosphorylation of Rab10 (Fig. 2 *J*–*L*), suggesting that lysosomal overload increased Rab10 phosphorylation by LRRK2.

Rab7L1 Is an Upstream Adaptor to Facilitate Lysosomal Translocation of LRRK2. We next explored the upstream molecular machinery that recruits LRRK2 onto overloaded lysosomes. Previous studies showed that Rab7L1 works as an interactor with LRRK2 in the regulation of intracellular trafficking (15, 42), and that Rab7L1 recruited LRRK2 to the *trans*-Golgi network (22, 23). We thus tested whether Rab7L1 induces LRRK2 translocation to overloaded lysosomes. We found that, in the absence of exogenous expression of LRRK2, Rab7L1 was recruited onto the lysosomes upon exposure to CQ (Fig. 3*A*). Before CQ treatment, Rab7L1 was mainly localized to the Golgi complex (*SI Appendix*, Fig. S3*D*), as reported (15, 43). Upon coexpression with LRRK2, both Rab7L1 and LRRK2 were translocated onto enlarged lysosomes upon CQ exposure (Fig. 3*B*), and the translocation of LRRK2 was dramatically enhanced by the coexpression of Rab7L1 (Fig. 3*C*). These lysosomes containing Rab7L1 and LRRK2 were not positive for markers of the Golgi, endoplasmic reticulum, or early endosomes (*SI Appendix*, Fig. S3*D*). Biochemical fractionation of purified lysosomes confirmed that Rab7L1 coexpression increased the lysosomal localization of LRRK2 in CQ-treated HEK293 cells (Fig. 3*D*). In contrast, knockdown of endogenous Rab7L1 in RAW264.7 cells significantly suppressed the translocation of endogenous LRRK2 onto enlarged lysosomes (Fig. 3 *E* and *F*). RNAi knockdown of the closest Rab members, Rab32 or Rab38, had no effect on the recruitment of LRRK2 (Fig. 3*F*), although Rab32 and Rab38 were translocated to lysosomes upon CQ treatment (*SI Appendix*, Fig. S3*E*). These results suggest that Rab7L1 acts as a specific upstream adaptor that recruits LRRK2 to the enlarged lysosomes.

LRRK2 Stabilizes Rab8a and Rab10 on LRRK2-Positive Enlarged Lysosomes in a Kinase Activity-Dependent Manner. We then sought to determine the downstream machinery of Rab7L1-LRRK2 recruitment on overloaded lysosomes. Since LRRK2 phosphorylates a subset of

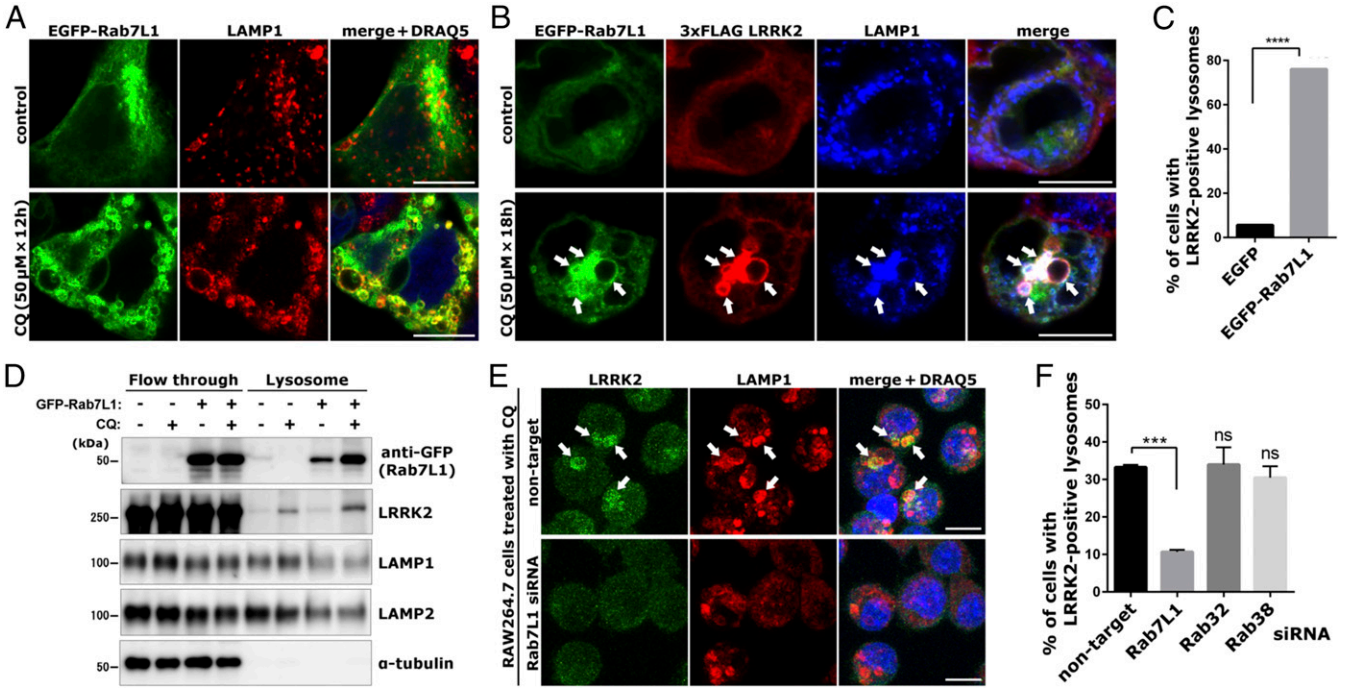

Fig. 3. Rab7L1 recruits LRRK2 onto the enlarged lysosomes. (*A*) Immunocytochemical analysis of the localization of EGFP-Rab7L1 in HEK293 cells with or without CQ treatment (50 μM, 18 h). (Scale bars: 10 μm.) (*B*) Immunocytochemical analysis of HEK293 cells coexpressing EGFP-Rab7L1 and 3× FLAG-LRRK2 with or without CQ treatment (50 μM, 18 h). Arrows indicate Rab7L1-LRRK2 double-positive lysosomes. (Scale bars: 10 μm.) (*C*) Percentage of cells harboring LRRK2-positive lysosomes, as shown in *B*, was statistically analyzed in LRRK2-expressing HEK293 cells coexpressing EGFP or EGFP-Rab7L1, with CQ treatment (n = 86 and n = 113 cells, respectively). ****$P < 0.0001$, Fisher's exact test. (*D*) Levels of Rab7L1, LRRK2, and control proteins in the lysosomal fraction analyzed by immunoblotting. Lysosomes were isolated from HEK293 cells that expressed 3× FLAG-LRRK2 and GFP-Rab7L1 with or without CQ treatment (50 μM, 24 h). (*E*) Lysosomal localization of LRRK2 in RAW264.7 cells treated with Rab7L1 siRNA and CQ (50 μM, 3 h). (Scale bars: 10 μm.) (*F*) Percentage of cells harboring endogenous LRRK2-positive lysosomes, as shown in *E*, analyzed in RAW264.7 cells treated with the indicated siRNA and CQ. Mean ± SEM (n = 3, 444–550 cells were analyzed in each experiment). ***$P < 0.001$, one-way ANOVA with Tukey's test. ns, not significant.

Rab GTPases in cells (22, 24–26) and phosphorylation occurs in the switch II region of Rab GTPases that mediates the binding with interactors responsible for vesicle transport, we screened for Rab GTPases that are coaccumulated on LRRK2-positive enlarged lysosomes.

We initially selected a total of 27 Rab GTPases (*SI Appendix*, Fig. S4), based on the presence of the Ser/Thr residue whose position is structurally equivalent to Thr72 of Rab8a, a phosphorylation site by LRRK2. We selected mostly one isoform per each Rab subclass, considering the similarity in structures and functions. We transfected HEK293 cells stably expressing wild-type (WT) or kinase-dead (K1906M) LRRK2 with each GFP-tagged Rab GTPase, treated cells with CQ for 24 h, and examined the localization of each GFP-Rab protein on LRRK2-positive lysosomes. We selected 10 Rab GTPases that were colocalized on LRRK2-positive lysosomes in cells expressing WT LRRK2 and treated with CQ, using the criterion that strong fluorescence of GFP-Rab is observed in >50% of LRRK2-positive lysosomes in >100 cells expressing each Rab protein (*SI Appendix*, Fig. S5 and Table S1). Six Rabs (Rab7, Rab9, Rab12, Rab17, Rab7L1, and Rab37) were excluded because their localization on LRRK2-positive lysosomes was similarly observed in cells expressing K1906M LRRK2 (*SI Appendix*, Fig. S5 and Table S1). Accordingly, Rab3a, Rab8a, Rab10, and Rab35 were identified as a class of Rab proteins that are localized on LRRK2-positive lysosomes upon CQ treatment in a manner dependent on the kinase activity of LRRK2 (*SI Appendix*, Fig. S5 and Table S1).

We then investigated the localization of endogenous Rab8a and Rab10 in RAW264.7 cells treated with CQ, as these Rab proteins were expected to be highly expressed in RAW264.7 cells (BioGPS portal, biogps.org/#goto=welcome). Endogenous Rab8a and Rab10 were detected on enlarged lysosomes upon CQ treatment, and colocalized with endogenous LRRK2 (Fig. 4 *A–D* and *SI Appendix*, Fig. S6*A*). The ratio of Rab8a-positive lysosomes relative to all lysosomes was ∼30% (Fig. 4*B*), and nearly all LRRK2-positive lysosomes were Rab8a-positive (Fig. 4*D*). Treatment with either of the LRRK2 kinase inhibitors, GSK2578215A or PF-06447475, almost completely suppressed the translocation of Rab8a and Rab10 onto LRRK2-positive enlarged lysosomes (Fig. 4 *A–D* and *SI Appendix*, Fig. S6*A*), without affecting the translocation of LRRK2 per se (Fig. 4*C*). In contrast, triple knockdown of Rab8a, Rab8b, and Rab10 did not suppress the lysosomal targeting of LRRK2 (*SI Appendix*, Fig. S6 *B* and *C*). Other treatments that induce LRRK2 translocation (e.g., zymosan treatment, long exposure to BafA1) also caused Rab8a accumulation on LRRK2-positive lysosomes (*SI Appendix*, Fig. S6 *D* and *E*). Biochemical analysis of purified lysosomes from LRRK2-expressing HEK293 cells validated the CQ-induced increase of endogenous Rab8a or Rab10 in the lysosome fraction (*SI Appendix*, Fig. S6*F*). These results suggest that lysosomal overload stress induces translocation of Rab8a and Rab10 onto enlarged lysosomes in an LRRK2 kinase activity-dependent manner.

As Thr72 of Rab8a and Thr73 of Rab10 have been identified as the phosphorylation sites by LRRK2 (24), we then examined the translocation of nonphosphorylatable Rab8a (T72A) and Rab10 (T73A). These mutants were not localized on LRRK2-positive enlarged lysosomes (Fig. 4 *E* and *F* and *SI Appendix*, Fig. S6*G*), suggesting that the phosphorylation of Rab8a or Rab10 at these sites is required for its lysosomal translocation. The lack of the lysosomal localization of nonphosphorylatable mutants was not due to the loss of GEF-mediated activation, because WT and

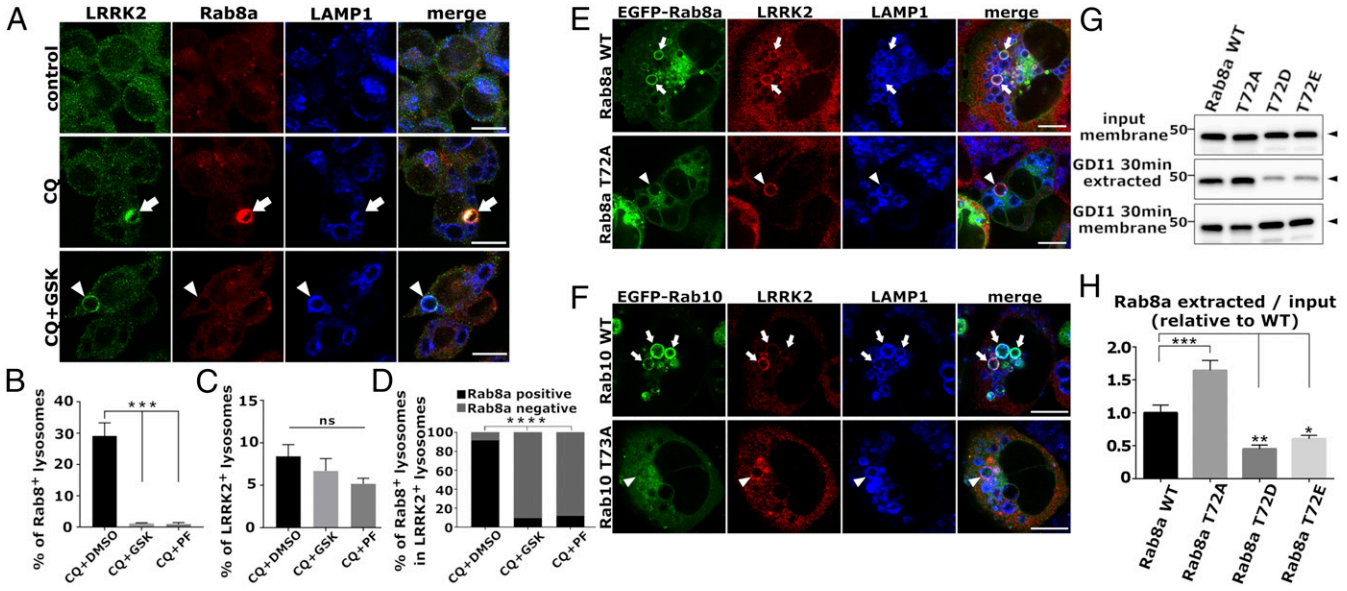

Fig. 4. Rab8a and Rab10 were accumulated on enlarged lysosomes through phosphorylation by LRRK2. (*A*) Immunocytochemical analysis of the localization of endogenous Rab8a in RAW264.7 cells without CQ treatment (*Top*), with CQ treatment (*Middle*), or treatment with CQ plus LRRK2 kinase inhibitor GSK2578215A (*Bottom*) using anti-LRRK2 (N138/6) and anti-Rab8a (ERP14873) antibodies. Arrows indicate LRRK2/Rab double-positive lysosomes, and arrowheads indicate LRRK2-positive, Rab-negative lysosomes. (Scale bars: 10 μm.) (*B* and *C*) Percentages of Rab8-positive (*B*) or LRRK2-positive (*C*) lysosomes in total enlarged lysosomes analyzed in cells exposed to CQ and LRRK2 inhibitors, as shown in *A*. Data represent mean ± SEM ($n = 3$, 93–151 lysosomes were analyzed in each experiment). ***$P < 0.001$, one-way ANOVA with Tukey's test. ns, not significant. (*D*) Percentages of Rab8-positive lysosomes that comprise the total LRRK2-positive lysosomes. A total of 37, 21, and 17 LRRK2-positive lysosomes were analyzed in each condition. ****$P < 0.0001$, Fisher's exact test. (*E* and *F*) Accumulation of Rab8a and Rab10 on enlarged lysosomes in HEK293 cells coexpressing 3× FLAG-LRRK2 (WT) and EGFP-Rab8a (*E*, WT or T72A) or EGFP-Rab10 (*F*, WT or T73A) and treated with CQ. Arrows indicate LRRK2/Rab double-positive lysosomes, and arrowheads indicate LRRK2-positive, Rab-negative lysosomes. (Scale bars: 10 μm.) (*G* and *H*) GDI-mediated extraction of Rab8a from membranes. Membrane fractions from HEK293 cells overexpressing GFP-Rab8a (WT, phosphomimetic mutants) were incubated with purified GDI1 for 30 min, and ultracentrifuged; Rab8a in supernatant ("extracted") was analyzed by immunoblotting with an anti-GFP antibody. The amount of Rab8a in the extracted fraction was divided by that of Rab8a in the input membrane fraction and normalized by the value in the Rab8a WT sample. Mean ± SEM ($n = 4$). *$P < 0.05$, **$P < 0.01$, ***$P < 0.001$; one-way ANOVA with Tukey's test.

CELL BIOLOGY

mutant forms of Rab8a or Rab10 were similarly activated in cells by their GEF, Rabin8, as assessed by the pulldown experiment using a C-terminal fragment of MICAL-L2 that selectively traps GTP-bound active forms of Rab8a or Rab10 (44) (*SI Appendix*, Fig. S6 *H* and *I*).

As the targeting of Rab proteins to cellular membranes is known to be regulated by their specific GEFs (45), we examined the involvement of the two Rab8a GEFs (Rabin8 and GRAB) in the phosphorylation-dependent Rab8a accumulation on lysosomes. Knockdown of neither of the GEFs prevented the Rab8a accumulation on lysosomes (*SI Appendix*, Fig. S7 *A* and *B*), and the colocalization of Rabin8 or GRAB on Rab8-positive lysosomes also was hardly detectable (*SI Appendix*, Fig. S7*C*), suggesting that these GEFs do not play a vital role in the targeting of Rab8a to enlarged lysosomes. On the other hand, we confirmed that phosphorylation of Rab GTPases by LRRK2 abolished the interaction of Rab with GDI1/2 (*SI Appendix*, Fig. S7*D*) as reported (24, 27), and further revealed that the phosphomimetic Rab8a and Rab10 (Rab8a T72D/E and Rab10 T73D/E, respectively) were resistant to extraction from membranes by purified GDI1 (Fig. 4 *G* and *H* and *SI Appendix*, Fig. S7*D*). These data support the notion that LRRK2-mediated phosphorylation stabilizes Rab GTPases on the lysosomal membranes by preventing GDI binding.

LRRK2 and Rab7L1 Regulate Lysosomal Enlargement and Secretion Induced by CQ Treatment. Next, we explored the downstream cellular effects of the lysosomal recruitment of LRRK2 and Rab GTPases. Knockdown of endogenous LRRK2 in RAW264.7 cells did not alter the lysosomal morphology in the absence of CQ treatment (Fig. 5*A*). However, knockdown of LRRK2 in CQ-treated cells dramatically enhanced the lysosomal enlargement (Fig. 5 *A* and *B*). The efficiency of LRRK2 knockdown was not altered by CQ treatment (*SI Appendix*, Fig. S8 *A* and *B*). In addition, treatment with the LRRK2 kinase inhibitors significantly enhanced the lysosomal enlargement upon CQ exposure (Fig. 5 *C* and *D*). Overexpression of WT LRRK2 in HEK293 cells significantly suppressed the enlargement of lysosomes upon

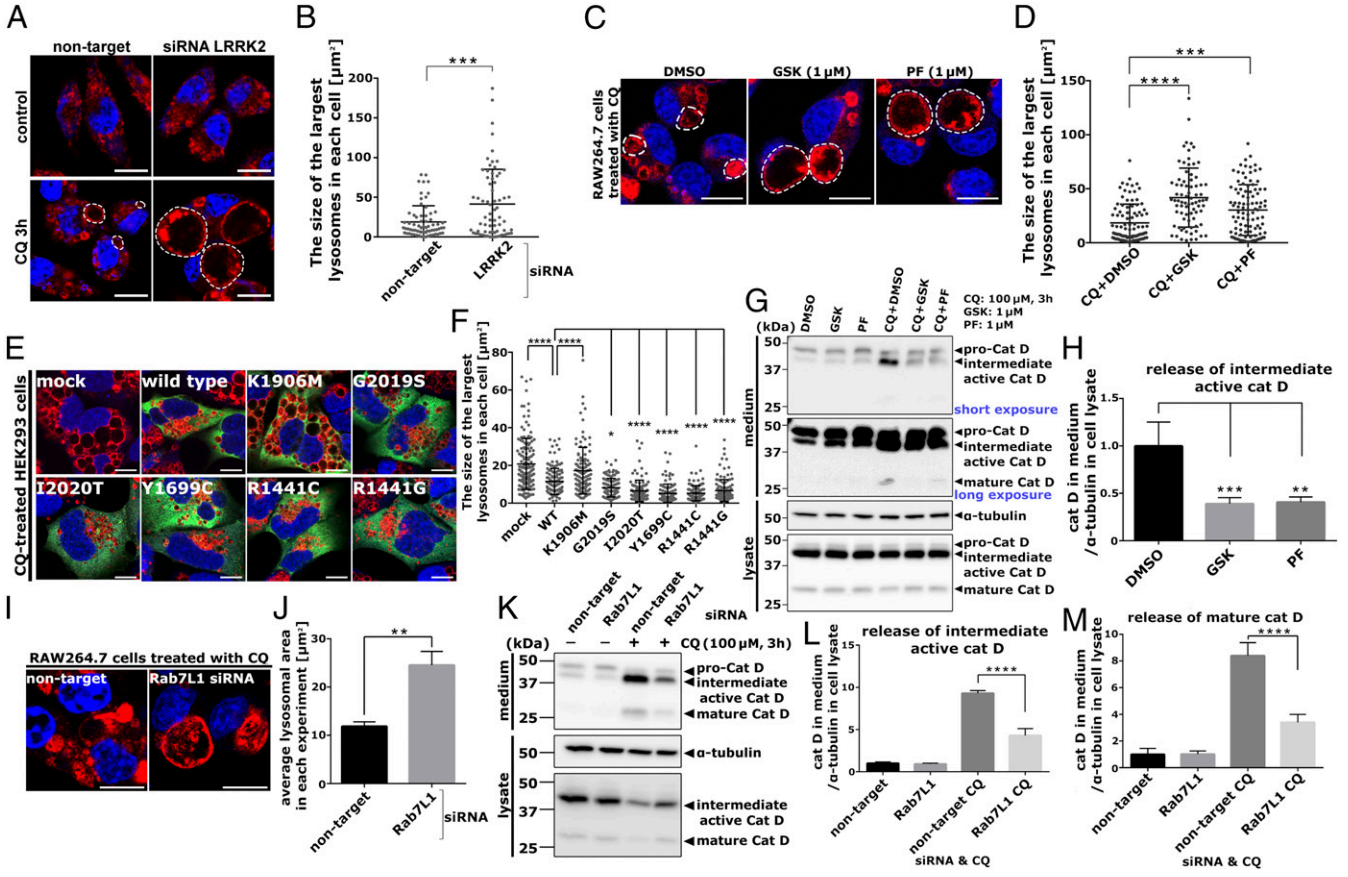

Fig. 5. LRRK2 and Rab7L1 regulate lysosomal morphology and lysosomal release upon CQ exposure. (*A*) Lysosomal morphology in RAW264.7 cells treated with LRRK2 siRNA and CQ (50 μM, 3 h). Cells were stained for LAMP1 (red) and nuclei (DRAQ5, blue). The largest lysosome in each cell was surrounded by a broken line. (Scale bars: 10 μm.) (*B*) Size of the largest lysosome in each cell, as examined in *A*. Mean ± SD ($n = 68$ and $n = 69$ for nontarget and LRRK2 RNAi, respectively). ***$P < 0.001$, *t* test. (*C*) Lysosomal morphology in cells treated with CQ in the presence of LRRK2 kinase inhibitors or DMSO. Red, LAMP1; blue, DRAQ5. (Scale bars: 10 μm.) (*D*) Size of the largest lysosome in each cell, as examined in *C*. Mean ± SD ($n = 96$, $n = 78$, and $n = 102$ for DMSO, GSK, and PF, respectively). ***$P < 0.001$, ****$P < 0.0001$; one-way ANOVA with Tukey's test. (*E*) Lysosomal morphology in HEK293 cells transfected with LRRK2 and treated with CQ (50 μM, 24 h). Red, LAMP1; green, LRRK2; blue, DRAQ5. (Scale bars: 10 μm.) (*F*) Size of the largest lysosome in each cell, as examined in *E*. Mean ± SD (178–211 cells in each condition). *$P < 0.05$, ****$P < 0.0001$; one-way ANOVA with Tukey's test. (*G*) Immunoblot analysis of the levels of cathepsin D (Cat D) species in media of RAW264.7 cells treated with LRRK2 inhibitors (GSK, PF) and/or CQ. (*H*) Densitometric analysis of the levels of intermediate active Cat D in media, as shown in *G*. Mean ± SD ($n = 4$). **$P < 0.01$, ***$P < 0.001$; one-way ANOVA with Tukey's test. (*I*) Lysosomal morphology in cells treated with Rab7L1 siRNA and CQ. Red, LAMP1; blue, DRAQ5. (Scale bars: 10 μm.) (*J*) Size of the largest lysosome in each cell, as examined in *I*. Mean ± SEM ($n = 4$, 105–163 cells in each experiment). **$P < 0.01$, *t* test. (*K*) Immunoblot analysis of the levels of Cat D in media of cells treated with nontarget or Rab7L1 siRNA and CQ. (*L* and *M*) Densitometric analysis of the levels of intermediate active (*L*) and mature (*M*) Cat D in media, as shown in *K*. Mean ± SD ($n = 4$). ****$P < 0.0001$, one-way ANOVA with Tukey's test.

CQ exposure (Fig. 5 *E* and *F*), whereas kinase-dead LRRK2 (K1906M) had no effects (Fig. 5 *E* and *F*). Furthermore, overexpression of the PD-associated mutant LRRK2 (i.e., R1441C, R1441G, Y1699C, G02019S, I2020T), which has been shown to increase the phosphorylation of Rab proteins (22, 24–26), altogether suppressed the lysosomal enlargement more efficiently than did WT LRRK2 (Fig. 5 *E* and *F*). These results support the notion that the stress-induced enlargement of lysosomes is regulated by the kinase activity of LRRK2.

Acute treatment with CQ has been shown to induce the lysosomal secretion along with its enlargement (46). We thus examined the effects of LRRK2 on the extracellular release of lysosomal contents upon CQ exposure. Treatment with either of the LRRK2 kinase inhibitors, GSK2578215A or PF-06447475, significantly suppressed the CQ-induced extracellular release of lysosomal enzyme proteins (i.e., mature cathepsin D, intermediate active cathepsin D, mature cathepsin B) from lysosomes (Fig. 5 *G* and *H* and *SI Appendix*, Fig. S8 *C–F*). Furthermore, the release of these lysosomal enzymes was not suppressed by brefeldin A, an inhibitor of conventional exocytosis via the Golgi (*SI Appendix*, Fig. S8 *C–F*). In contrast, the release of procathepsin B and D was not enhanced by CQ treatment but was inhibited by brefeldin A treatment (*SI Appendix*, Fig. S8 *C* and *G*), suggesting that procathepsins were released via the Golgi to the extracellular space. The CQ-induced release of lysosomal contents was not a result of cell death, as confirmed by the secretion of lactate dehydrogenase (LDH) into media (*SI Appendix*, Fig. S8*H*). Taken together, we concluded that the kinase activity of LRRK2 is involved in the lysosomal release upon lysosomal overload.

We also examined the effect of the upstream regulator Rab7L1 on lysosomal enlargement and release. Knockdown of Rab7L1 in RAW264.7 cells enhanced the CQ-induced enlargement of lysosomes (Fig. 5 *I* and *J*) and attenuated the lysosomal release (Fig. 5 *K–M*) without increasing LDH release (*SI Appendix*, Fig. S8*I*). These data supported the notion that the Rab7L1-LRRK2 pathway regulates the stress-induced lysosomal enlargement and secretion.

Rab8 and Rab10 Regulate CQ-Induced Lysosomal Enlargement and Secretion by Recruiting Their Effectors EHBP1 and EHBP1L1. We next examined the involvement of Rab8 and Rab10 in the CQ-induced lysosomal enlargement and secretion. Double knockdown of Rab8a/8b harboring redundant functions (46), as well as Rab8a/8b/10 triple knockdown, significantly enhanced the CQ-induced lysosomal enlargement (Fig. 6 *A* and *B*). In contrast, Rab10 knockdown did not enhance the enlargement of lysosomes (Fig. 6 *A* and *B*). Furthermore, coexpression of LRRK2 with Rab8a WT in HEK293 cells significantly suppressed lysosomal enlargement compared with that with Rab8a T72A (Fig. 6 *C* and *D*), underscoring the requirement of LRRK2-mediated phosphorylation. In contrast, CQ-induced extracellular release of lysosomal cathepsin D was suppressed by knockdown of Rab10, but not by that of Rab8a/8b (Fig. 6 *E–G* and *SI Appendix*, Fig. S9*A*). These results suggested that CQ-induced lysosomal enlargement and secretion were regulated by Rab8 and Rab10.

We further sought for the downstream effectors of Rab8/10 localized on lysosomes. We knocked down 14 known effectors of Rab8/10 (*SI Appendix*, Table S2) using siRNA with confirmed knockdown efficiencies (*SI Appendix*, Fig. S9 *D* and *E*) and analyzed the effects on lysosomal morphology and lysosomal release. Among the effectors analyzed, knockdown of EHBP1 and EHBP1L1 significantly enhanced lysosomal enlargement and suppressed lysosomal release upon CQ treatment (Fig. 6 *H–K* and *SI Appendix*, Fig. S9 *B–E*). We also found that endogenous EHBP1L1, as well as overexpressed EHBP1 and EHBP1L1, was accumulated on Rab8-positive enlarged lysosomes (Fig. 6*L* and *SI Appendix*, Fig. S9*F*). The ability of Rab8a to bind EHBP1L1 was not altered by the Rab8a phosphomimetic mutations (*SI Appendix*, Fig. S9*G*). These data suggest that EHBP1 and EHBP1L1 are the functional downstream effectors involved in lysosomal homeostasis.

LRRK2 Acts Against CQ-Induced Lysosomal Overload Stress in Vivo. We examined the potential role of endogenous LRRK2 on lysosomal overload stress in *Lrrk2* KO mice. Eighteen-month-old aged *Lrrk2* KO mice exhibited extensive vacuolization as well as an accumulation of autofluorescent lipofuscin and LAMP1-positive lysosomes in renal proximal tubule cells (Fig. 7*A* and *SI Appendix*, Fig. S10 *A* and *B*), as reported (11, 12, 47), whereas such pathologies were not evident in 8-wk-old young *Lrrk2* KO mice. To examine whether young *Lrrk2* KO mice exhibit vulnerability to lysosomal stresses, we administrated CQ i.p. in 8-wk-old young *Lrrk2* KO mice or heterozygous mice as controls daily for 2 wk. *Lrrk2* KO mice exhibited significant vacuolization, an increase in lipofuscin autofluorescence, and an enhancement of LAMP1 staining in renal proximal tubule cells (Fig. 7 *B–E*). These data suggested that LRRK2 functions against lysosomal overload stress in vivo, particularly in renal proximal tubules exposed to lysosomal stress.

Discussion

In this study, we revealed the cellular responses of LRRK2 and its target Rab GTPases to lysosomal overload stress. Endogenous LRRK2 was dynamically translocated onto the overloaded lysosomes and was activated. An upstream adaptor, Rab7L1, recruited LRRK2 to lysosomes, which, in turn, stabilized its substrates Rab8a and Rab10 on lysosomes through their phosphorylation; these Rab GTPases further recruited their effectors EHBP1 and EHBP1L1 to regulate lysosomal homeostasis. Our findings propose a molecular pathway composed of Rab7L1, LRRK2, phosphorylated Rab8/10, and their effectors in the control of lysosomal stress (Fig. 8*A*).

Our family-wide screen of Rab GTPases revealed that Rab3, Rab8, Rab10, and Rab35 were targeted to the LRRK2-positive overloaded lysosomes in a manner dependent on LRRK2 kinase activity. Interestingly, this subset encompassed the Rab GTPases that were recently identified as substrates of LRRK2 (i.e., Rab3, Rab8, Rab10, Rab12, Rab7L1, Rab35, Rab43) (25), supporting the notion that LRRK2-mediated phosphorylation of Rab GTPases is closely linked to their roles in the lysosomal stress response. Our findings suggested that under stress conditions, phosphorylated Rab GTPases acquire novel functions within a specific subcellular compartment that are completely different from those under the steady-state conditions; it is possible that the roles of Rab8a/10 on stressed lysosomes are different from their physiological functions documented in recycling endosomes (48). We should also note that the ratio of Rab8a/10-positive enlarged lysosomes was moderate (i.e., ∼30% of total lysosomes), which may raise questions about the contribution of Rab against lysosomal stress; further analysis of the dynamic nature and temporal changes of Rab localization and function in stressed lysosomes may give us clues to the significance of LRRK2 and Rab8/10 in maintaining the integrity of lysosomes.

The precise mechanism whereby LRRK2 induces lysosomal accumulation of its substrate Rab GTPases remains to be determined. The localization of Rab GTPases is generally dependent on their GEFs (45). However, it is also likely that the lysosomal targeting of Rab GTPases requires both GEF activity and their phosphorylation, because (*i*) nonphosphorylatable Rab8a and Rab10 (i.e., Rab8a-T72A, Rab10-T73A) were capable of being activated by their GEF Rabin8 but were not targeted onto the enlarged lysosomes, and (*ii*) Rab8/10 on stressed lysosomes may contain the GTP-bound active form, as the effectors EHBP1 and EHBP1L1 were coaccumulated with Rab8a on enlarged lysosomes. A possible determinant of the lysosomal anchoring of Rab GTPases through phosphorylation would be GDI, as shown by our results that Rab8a/10 phosphomimetics

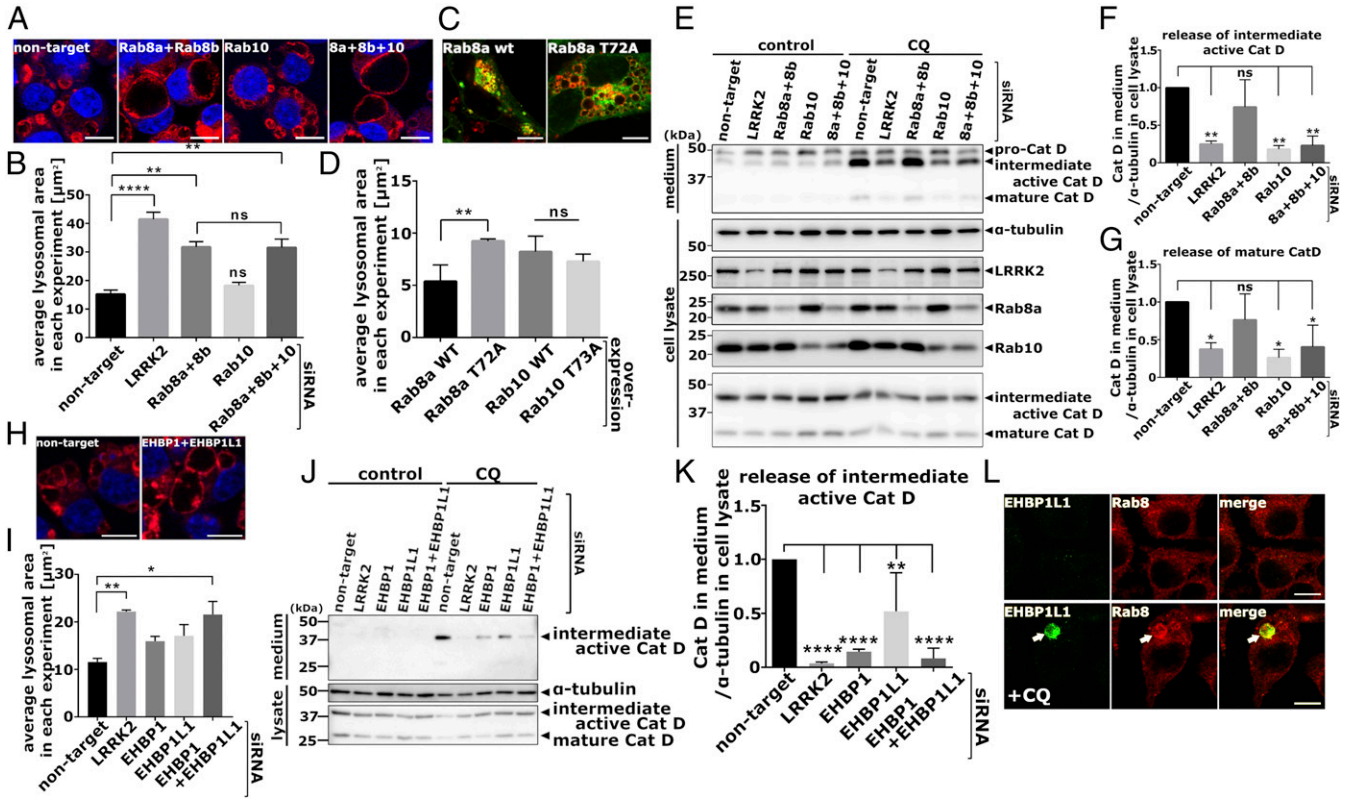

Fig. 6. Rab8, Rab10, and their effectors regulate lysosomal morphology and lysosomal release upon CQ exposure. (*A* and *B*) Lysosomal enlargement in RAW264.7 cells treated with siRNA against nontarget, LRRK2, Rab8a, Rab8b, or Rab10 and CQ (100 μM, 3 h). Red, LAMP1; blue, DRAQ5. (Scale bars: 10 μm.) Statistical analysis of the average size of the largest lysosomes in each cell is shown in *B*. Mean ± SEM ($n = 3$, 107–167 cells were analyzed in each experiment). $^{**}P < 0.01$, $^{***}P < 0.001$, $^{****}P < 0.0001$; one-way ANOVA with Tukey's test. ns, not significant. (*C* and *D*) Lysosomal enlargement in HEK293 cells coexpressing 3× FLAG-LRRK2 and Rab8a (WT, T72A) or Rab10 (WT, T73A) treated with CQ (50 μM, 24 h). (Scale bars: 10 μm.) Statistical analysis of the average size of the largest lysosomes in each cell is shown in *D*. Mean ± SEM ($n = 5$, 109–140 cells were analyzed in each experiment). $^{**}P < 0.01$, one-way ANOVA with Tukey's test. (*E*) Immunoblot analysis of the levels of cathepsin D (Cat D) species in media of RAW264.7 cells treated with the indicated siRNA and CQ (100 μM, 3 h). (*F* and *G*) Densitometric analysis of the levels of intermediate active (*F*) or mature (*G*) Cat D in media, as shown in *E*. Mean ± SD ($n = 3$). $^{*}P < 0.05$, $^{**}P < 0.01$; one-way ANOVA with Tukey's test. (*H* and *I*) Lysosomal enlargement in RAW264.7 cells treated with siRNA against EHBP1, EHBP1L1, or both and CQ (100 μM, 3 h). Doubly treated representative cells are shown in *H*. Red, LAMP1; blue, DRAQ5. (Scale bars: 10 μm.) Average size of the largest lysosomes in each cell is shown in *I*. Mean ± SEM ($n = 3$, 75–142 cells in each experiment). $^{*}P < 0.05$, $^{**}P < 0.01$; one-way ANOVA with Tukey's test. (*J*) Immunoblot analysis of the levels of Cat D species in media of RAW264.7 cells treated with siRNA against EHBP1, EHBP1L1, or both and CQ (100 μM, 3 h). (*K*) Densitometric analysis of the levels of intermediate active Cat D in media as shown in *J*. Mean ± SEM ($n = 4$). $^{**}P < 0.01$, $^{****}P < 0.0001$; one-way ANOVA with Tukey's test. (*L*) Localization of endogenous EHBP1L1 in RAW264.7 cells treated without CQ (*Top*) or with CQ (*Bottom*). Arrows indicate EHBP1L1 on Rab8-positive enlarged lysosomes. (Scale bars: 10 μm.)

were resistant to the extraction from membranes by purified GDI1, which was in agreement with previous data showing the loss of interaction between phosphorylated Rab8a/10 and GDI1/2 in cells (24, 49, 50). Based on these data, we propose a putative mechanism for the maintenance of lysosomal homeostasis by LRRK2 and Rab GTPases. Upon exposure to lysosomal overload stress, Rab7L1, LRRK2, and phosphorylated Rab8/10 are sequentially accumulated onto the stressed lysosomes, which then promotes the release of lysosomal contents and suppresses the lysosomal enlargement through their effectors, EHBP1 and EHBP1L1 (Fig. 8*A*). The phosphorylated Rab8/10 on lysosomal membranes remains resistant to the extraction from membranes by GDI, thereby accumulating on lysosomes; Rab8/10 may then be activated by GEFs and recruit their effectors (Fig. 8*B*). However, there still remain a number of uncertain points in the current model of Rab regulation, which we should address by further elucidating the mechanism of phosphorylation-dependent translocation or stabilization of Rab in relation to the specific interactors.

We have revealed that LRRK2 and its target Rabs regulate two distinct types of lysosomal responses (lysosomal enlargement and lysosomal release). Elevated lysosomal enlargement causes lysosomal membrane permeabilization that leads to cell death (51), whereas defective lysosomal exocytosis is implicated in lysosomal storage disorders (52, 53). Thus, LRRK2 and target Rab GTPases may counteract against such deteriorative stresses, prompting us to determine the effects of LRRK2/Rab on downstream lysosomal functions (e.g., digestion of lysosomal substrates, luminal pH maintenance). We also need to reveal the mechanistic roles of EHBP1 and EHBP1L1, two functional Rab8/10 effectors implicated in lysosomal maintenance. Prior studies reported that EHBP1 on endosomes promotes endosomal tubulation through binding to the actin cytoskeleton (54) and that EHBP1L1 functions with Bin1 to generate membrane curvature to excise the vesicle at the endocytic recycling compartment (48). Thus, it is tempting to speculate that EHBP1 and EHBP1L1 promote vesicle formation and budding on lysosomal membranes to maintain the morphology and function of the stressed lysosomes.

Our data using *Lrrk2* KO mice exposed to CQ support the notion that LRRK2 alleviates lysosomal overload stress in vivo. Lysosome overload may increase with age (55, 56), as represented by an intralysosomal accumulation of lipofuscin, which was also observed in aged *Lrrk2* KO mice; collectively, these data

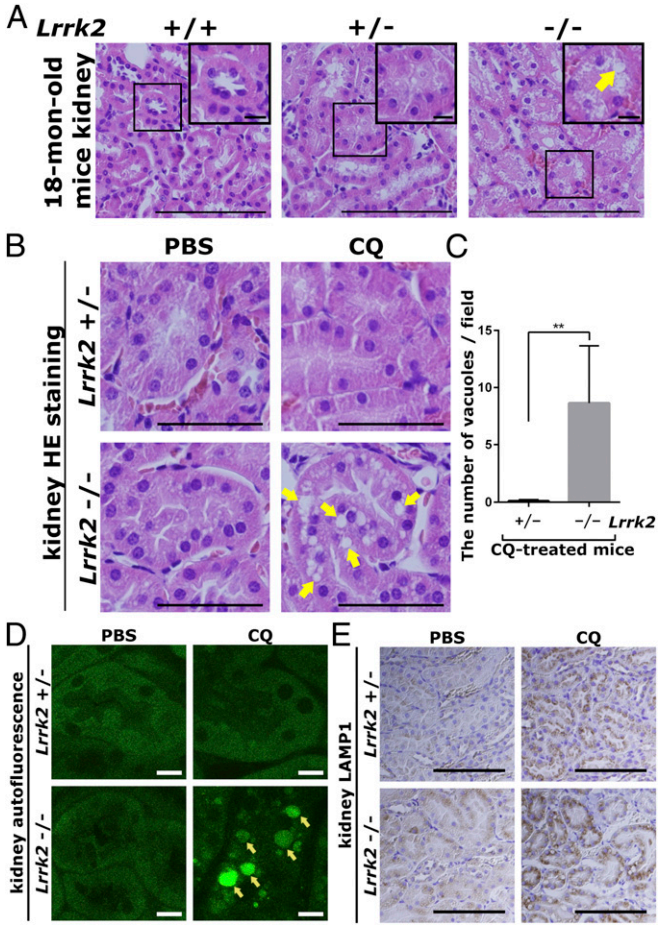

Fig. 7. LRRK2 deficiency confers vulnerability to lysosomal stress on renal tubular cells in vivo. (*A*) Hematoxylin and eosin (HE) staining of renal proximal tubules from 18-mo-old *Lrrk2* KO mice and control mice. (*Insets*, *Top Right*) Magnified images of the boxed areas. The arrow indicates the vacuoles formed in $Lrrk2^{-/-}$ mice. (Scale bars: 100 μm; *Insets*, 10 μm.) (*B*) HE staining of renal proximal tubules from 8-wk-old mice injected i.p. with CQ for 2 wk. Arrows indicate the vacuoles formed in $Lrrk2^{-/-}$ mice administered CQ. (Scale bars: 50 μm.) (*C*) Quantification of the number of vacuoles in HE-stained renal proximal tubules of CQ-treated mice, as shown in *B*. Data represent mean ± SD (n = 5). $^{**}P < 0.01$, t test. (*D*) Autofluorescence in renal proximal tubules. Arrows indicate the autofluorescence in $Lrrk2^{-/-}$ mice administered CQ. (Scale bars: 10 μm.) (*E*) Immunostaining of renal proximal tubules from CQ-administered mice with an anti-LAMP1 antibody. (Scale bars: 100 μm.)

may suggest that LRRK2 is involved in alleviation of the age-dependent cumulative lysosomal impairment. Our observations that a small number of enlarged lysosomes were LRRK2-positive in steady-state cells (*SI Appendix*, Fig. S1*A*) and that phagolysosomes in RAW264.7 cells ingested with zymosan were similarly decorated with LRRK2 (Fig. 2*I*) support the physiological relevance of the roles of LRRK2 in lysosomes.

How LRRK2 and its target Rab are involved in neurodegeneration remains to be explored. Our present data that all PD-associated LRRK2 mutants constantly suppressed CQ-induced lysosomal enlargement is not consistent with the idea that LRRK2 mutation leads to susceptibility to PD by lowering protection against lysosomal stress. Alternatively, up-regulation of LRRK2-mediated lysosomal secretion may cause non–cell-autonomous deteriorations (e.g., an increase in the release of toxic α-synuclein aggregates), thereby aggravating neurodegeneration in PD.

In sum, we have revealed a mechanism of the lysosomal stress-responsive pathway involving LRRK2 and its target Rab GTPases through phosphorylation. Further studies on this pathway will pave the way toward a new understanding of the cell biology of lysosomes, as well as the disease mechanisms.

Materials and Methods

Cell Culture and Transfection. HEK293 cells, HEK293A cells, and 3T3-Swiss albino cells were cultured in DMEM supplemented with 10% (vol/vol) FBS and in 100 units/mL penicillin and 100 μg/mL streptomycin at 37 °C in a 5% CO_2 atmosphere. RAW264.7 cells (American Type Culture Collection) and MG6 cells (provided by Taisuke Tomita, The University of Tokyo) were cultured on culture dishes for suspended cells (Sumitomo Bakelite Co.) under the same condition as for the culture of HEK293 cells. RAW264.7 cells and MG6 cells were activated by IFN-γ treatment for 48 h before each assay. Transfection of plasmids and siRNA was performed using Lipofectamine LTX (Thermo Fisher Scientific) and Lipofectamine RNAiMAX (Thermo Fisher Scientific), respectively, according to the manufacturer's protocols. Cells were analyzed 72 h after siRNA transfection. For immunocytochemistry, cells were reseeded on a coverslip on the following day after transfection.

Morphometric Analysis of Lysosomes. Cells were treated with CQ (50 μM or 100 μM) for 3 h (RAW264.7 cells) or 18–24 h (HEK293 cells), as indicated. Lysosomes were fluorescence-stained with an anti-LAMP1 antibody. Images of cells were acquired using a confocal microscope. The area of the largest lysosome in each cell was measured using ImageJ (NIH) software and shown in dot plots. The average size of the largest lysosomes in each condition was calculated, and mean values of the average from three to five independent experiments were shown in bar graphs. A total of 68–211 cells on a coverslip were analyzed for each condition in each experiment.

Measurement of Cathepsin B/D and LDH in Media. IFN-γ–activated RAW264.7 cells were cultured in DMEM (without phenol red) containing 1% FBS for 3 h. Some cells were cultured in the presence of CQ (100 μM), GSK2578215A

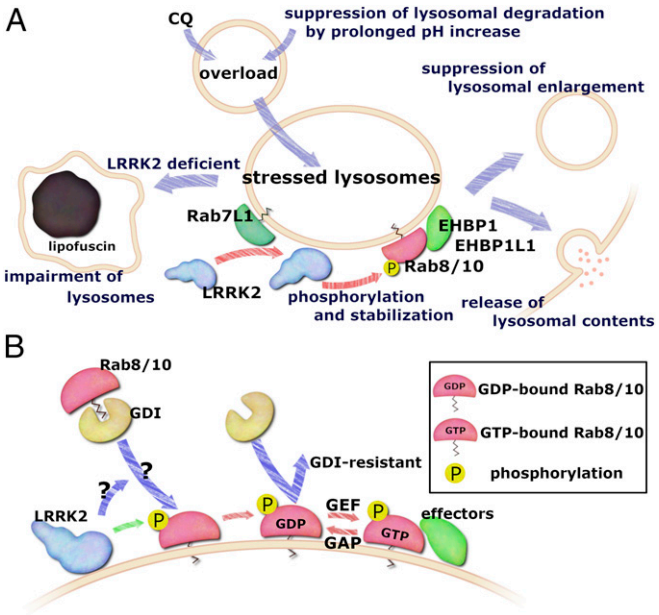

Fig. 8. Proposed model for the lysosomal stress response involving Rab7L1, LRRK2, and Rab8/10. (*A*) Maintenance of lysosomal homeostasis by LRRK2 and Rab GTPases. Within cells exposed to lysosomal overload stress, Rab7L1 is translocated from the Golgi to lysosomal membranes and recruits LRRK2 onto the stressed lysosomes. Translocated LRRK2 then stabilizes its substrates Rab8 and Rab10 on lysosomes depending on their phosphorylation. These Rab GTPases promote the release of lysosomal contents and suppress lysosomal enlargement through their effectors, EHBP1 and EHBP1L1. (*B*) Possible mechanism of Rab8/10 accumulation on lysosomal membranes. Rab8/10 is recruited onto lysosomal membranes and phosphorylated by LRRK2. The phosphorylated Rab8/10 remains resistant to the extraction from membranes by GDI, resulting in the accumulation on lysosomes. The accumulated Rab8/10 is then activated by GEFs and recruits their effectors.

CELL BIOLOGY

(1 μM), PF-06447475 (1 μM), or Brefeldin A (1 μM) for 3 h. Media were collected and centrifuged at 200 × *g* for 5 min. Cells were lysed and analyzed by immunoblotting. Supernatants of media were analyzed by immunoblotting and LDH assay. For immunoblotting, the supernatants were mixed with NuPAGE LDS Sample Buffer (4×) buffer (Thermo Fisher Scientific). The activity of LDH in the supernatants was measured using a Cytotoxicity Detection Kit (Roche Applied Science) according to the manufacturer's protocol.

CQ Treatment of Mice. All experiments with mice were performed in accordance with the regulations and guidelines of The University of Tokyo and were approved by The University of Tokyo Institutional Review Committee. *Lrrk2* KO mice (KO1, targeting the promoter and exon 1 region) (11) were provided by Jie Shen, Brigham and Women's Hospital, Boston. Eight-week-old mice were injected i.p. with 50 mg/kg (of body weight) of CQ diphosphate salt dissolved in PBS, or with PBS as a control, daily for 2 wk. Preparation and analysis of paraffin sections are described in *SI Appendix*.

Additional materials and methods are described in *SI Appendix*, *SI Materials and Methods*.

ACKNOWLEDGMENTS. We thank Dr. Jie Shen for providing *Lrrk2* KO mice; Yuko Matsuo and Paula Ackermann for their help in the Rab screening; Dr. Zen-ichi Tanei for the evaluation of mouse pathology; and Dr. Shogo Kamikawaji, Dr. Keisuke Wakasugi, and our laboratory members for helpful discussions. This work was supported by GlaxoSmithKline (GSK) Japan Research Grant 2015; Japan Society for the Promotion of Science KAKENHI Grants 16K07039, 26870114, 16J05538, and JP16H06280, a Grant-in-Aid for Scientific Research on Innovative Areas-Platforms for Advanced Technologies and Research Resources "Advanced Bioimaging Support."

1. Paisán-Ruíz C, et al. (2004) Cloning of the gene containing mutations that cause PARK8-linked Parkinson's disease. *Neuron* 44:595–600.
2. Zimprich A, et al. (2004) Mutations in LRRK2 cause autosomal-dominant parkinsonism with pleomorphic pathology. *Neuron* 44:601–607.
3. Lill CM, et al.; 23andMe Genetic Epidemiology of Parkinson's Disease Consortium; International Parkinson's Disease Genomics Consortium; Parkinson's Disease GWAS Consortium; Wellcome Trust Case Control Consortium 2) (2012) Comprehensive research synopsis and systematic meta-analyses in Parkinson's disease genetics: The PDGene database. *PLoS Genet* 8:e1002548.
4. Barrett JC, et al.; NIDDK IBD Genetics Consortium; Belgian-French IBD Consortium; Wellcome Trust Case Control Consortium (2008) Genome-wide association defines more than 30 distinct susceptibility loci for Crohn's disease. *Nat Genet* 40:955–962.
5. Zhang FR, et al. (2009) Genomewide association study of leprosy. *N Engl J Med* 361: 2609–2618.
6. Li X, et al. (2007) Leucine-rich repeat kinase 2 (LRRK2)/PARK8 possesses GTPase activity that is altered in familial Parkinson's disease R1441C/G mutants. *J Neurochem* 103:238–247.
7. Biskup S, et al. (2007) Dynamic and redundant regulation of LRRK2 and LRRK1 expression. *BMC Neurosci* 8:102.
8. Gardet A, et al. (2010) LRRK2 is involved in the IFN-gamma response and host response to pathogens. *J Immunol* 185:5577–5585.
9. Martin I, Kim JW, Dawson VL, Dawson TM (2014) LRRK2 pathobiology in Parkinson's disease. *J Neurochem* 131:554–565.
10. Roosen DA, Cookson MR (2016) LRRK2 at the interface of autophagosomes, endosomes and lysosomes. *Mol Neurodegener* 11:73.
11. Tong Y, et al. (2010) Loss of leucine-rich repeat kinase 2 causes impairment of protein degradation pathways, accumulation of alpha-synuclein, and apoptotic cell death in aged mice. *Proc Natl Acad Sci USA* 107:9879–9884.
12. Herzig MC, et al. (2011) LRRK2 protein levels are determined by kinase function and are crucial for kidney and lung homeostasis in mice. *Hum Mol Genet* 20:4209–4223.
13. Hinkle KM, et al. (2012) LRRK2 knockout mice have an intact dopaminergic system but display alterations in exploratory and motor co-ordination behaviors. *Mol Neurodegener* 7:25.
14. Fuji RN, et al. (2015) Effect of selective LRRK2 kinase inhibition on nonhuman primate lung. *Sci Transl Med* 7:273ra15.
15. MacLeod DA, et al. (2013) RAB7L1 interacts with LRRK2 to modify intraneuronal protein sorting and Parkinson's disease risk. *Neuron* 77:425–439.
16. Gómez-Suaga P, et al. (2014) LRRK2 delays degradative receptor trafficking by impeding late endosomal budding through decreasing Rab7 activity. *Hum Mol Genet* 23:6779–6796.
17. Kuwahara T, et al. (2016) LRRK2 and RAB7L1 coordinately regulate axonal morphology and lysosome integrity in diverse cellular contexts. *Sci Rep* 6:29945.
18. Satake W, et al. (2009) Genome-wide association study identifies common variants at four loci as genetic risk factors for Parkinson's disease. *Nat Genet* 41:1303–1307.
19. Gan-Or Z, et al. (2012) Association of sequence alterations in the putative promoter of RAB7L1 with a reduced Parkinson disease risk. *Arch Neurol* 69:105–110.
20. Goudarzian M, et al. (2015) The rs1572931 polymorphism of the RAB7L1 gene promoter is associated with reduced risk of Parkinson's disease. *Neurol Res* 37:1029–1031.
21. Pihlstrøm L, et al. (2015) Fine mapping and resequencing of the PARK16 locus in Parkinson's disease. *J Hum Genet* 60:357–362.
22. Liu Z, et al. (2018) LRRK2 phosphorylates membrane-bound Rabs and is activated by GTP-bound Rab7L1 to promote recruitment to the trans-Golgi network. *Hum Mol Genet* 27:385–395.
23. Purlyte E, et al. (2018) Rab29 activation of the Parkinson's disease-associated LRRK2 kinase. *EMBO J* 37:1–18.
24. Steger M, et al. (2016) Phosphoproteomics reveals that Parkinson's disease kinase LRRK2 regulates a subset of Rab GTPases. *eLife* 5:e12813.
25. Steger M, et al. (2017) Systematic proteomic analysis of LRRK2-mediated Rab GTPase phosphorylation establishes a connection to ciliogenesis. *eLife* 6:e31012.
26. Fujimoto T, et al. (2018) Parkinson's disease-associated mutant LRRK2 phosphorylates Rab7L1 and modifies trans-Golgi morphology. *Biochem Biophys Res Commun* 495:1708–1715.
27. Madero-Pérez J, et al. (2018) Parkinson disease-associated mutations in LRRK2 cause centrosomal defects via Rab8a phosphorylation. *Mol Neurodegener* 13:3.
28. West AB, et al. (2005) Parkinson's disease-associated mutations in leucine-rich repeat kinase 2 augment kinase activity. *Proc Natl Acad Sci USA* 102:16842–16847.
29. Biskup S, et al. (2006) Localization of LRRK2 to membranous and vesicular structures in mammalian brain. *Ann Neurol* 60:557–569.
30. Hatano T, et al. (2007) Leucine-rich repeat kinase 2 associates with lipid rafts. *Hum Mol Genet* 16:678–690.
31. Kett LR, et al. (2012) LRRK2 Parkinson disease mutations enhance its microtubule association. *Hum Mol Genet* 21:890–899.
32. Diettrich O, Mills K, Johnson AW, Hasilik A, Winchester BG (1998) Application of magnetic chromatography to the isolation of lysosomes from fibroblasts of patients with lysosomal storage disorders. *FEBS Lett* 441:369–372.
33. Lee JH, et al. (2015) Presenilin 1 maintains lysosomal Ca(2+) homeostasis via TRPML1 by regulating vATPase-mediated lysosome acidification. *Cell Rep* 12:1430–1444.
34. Cerny J, et al. (2004) The small chemical vacuolin-1 inhibits Ca(2+)-dependent lysosomal exocytosis but not cell resealing. *EMBO Rep* 5:883–888.
35. Kurz T, Terman A, Gustafsson B, Brunk UT (2008) Lysosomes and oxidative stress in aging and apoptosis. *Biochim Biophys Acta* 1780:1291–1303.
36. Reeves EP, et al. (2002) Killing activity of neutrophils is mediated through activation of proteases by K+ flux. *Nature* 416:291–297.
37. Florey O, Gammoh N, Kim SE, Jiang X, Overholtzer M (2015) V-ATPase and osmotic imbalances activate endolysosomal LC3 lipidation. *Autophagy* 11:88–99.
38. Ito G, et al. (2016) Phos-tag analysis of Rab10 phosphorylation by LRRK2: A powerful assay for assessing kinase function and inhibitors. *Biochem J* 473:2671–2685.
39. Kinoshita E, Kinoshita-Kikuta E, Takiyama K, Koike T (2006) Phosphate-binding tag, a new tool to visualize phosphorylated proteins. *Mol Cell Proteomics* 5:749–757.
40. Reith AD, et al. (2012) GSK2578215A; a potent and highly selective 2-arylmethyloxy-5-substitutent-N-arylbenzamide LRRK2 kinase inhibitor. *Bioorg Med Chem Lett* 22: 5625–5629.
41. Henderson JL, et al. (2015) Discovery and preclinical profiling of 3-[4-(morpholin-4-yl)-7H-pyrrolo[2,3-d]pyrimidin-5-yl]benzonitrile (PF-06447475), a highly potent, selective, brain penetrant, and in vivo active LRRK2 kinase inhibitor. *J Med Chem* 58:419–432.
42. Beilina A, et al.; International Parkinson's Disease Genomics Consortium; North American Brain Expression Consortium (2014) Unbiased screen for interactors of leucine-rich repeat kinase 2 supports a common pathway for sporadic and familial Parkinson disease. *Proc Natl Acad Sci USA* 111:2626–2631.
43. Wang S, et al. (2014) A role of Rab29 in the integrity of the trans-Golgi network and retrograde trafficking of mannose-6-phosphate receptor. *PLoS One* 9:e96242.
44. Homma Y, Fukuda M (2016) Rabin8 regulates neurite outgrowth in both GEF activity-dependent and -independent manners. *Mol Biol Cell* 27:2107–2118.
45. Blümer J, et al. (2013) RabGEFs are a major determinant for specific Rab membrane targeting. *J Cell Biol* 200:287–300.
46. Goldman SD, Krise JP (2010) Niemann-Pick C1 functions independently of Niemann-Pick C2 in the initial stage of retrograde transport of membrane-impermeable lysosomal cargo. *J Biol Chem* 285:4983–4994.
47. Tong Y, et al. (2012) Loss of leucine-rich repeat kinase 2 causes age-dependent bi-phasic alterations of the autophagy pathway. *Mol Neurodegener* 7:2.
48. Nakajo A, et al. (2016) EHBP1L1 coordinates Rab8 and Bin1 to regulate apical-directed transport in polarized epithelial cells. *J Cell Biol* 212:297–306.
49. Levin RS, Hertz NT, Burlingame AL, Shokat KM, Mukherjee S (2016) Innate immunity kinase TAK1 phosphorylates Rab1 on a hotspot for posttranslational modifications by host and pathogen. *Proc Natl Acad Sci USA* 113:E4776–E4783.
50. Shinde SR, Maddika S (2016) PTEN modulates EGFR late endocytic trafficking and degradation by dephosphorylating Rab7. *Nat Commun* 7:10689.
51. Ono K, Kim SO, Han J (2003) Susceptibility of lysosomes to rupture is a determinant for plasma membrane disruption in tumor necrosis factor alpha-induced cell death. *Mol Cell Biol* 23:665–676.
52. Medina DL, et al. (2011) Transcriptional activation of lysosomal exocytosis promotes cellular clearance. *Dev Cell* 21:421–430.
53. Cao Q, et al. (2015) BK channels alleviate lysosomal storage diseases by providing positive feedback regulation of lysosomal Ca2+ release. *Dev Cell* 33:427–441.
54. Wang P, et al. (2016) RAB-10 promotes EHBP-1 bridging of filamentous actin and tubular recycling endosomes. *PLoS Genet* 12:e1006093.
55. Cuervo AM, Dice JF (2000) When lysosomes get old. *Exp Gerontol* 35:119–131.
56. Settembre C, Fraldi A, Medina DL, Ballabio A (2013) Signals from the lysosome: A control centre for cellular clearance and energy metabolism. *Nat Rev Mol Cell Biol* 14: 283–296.